Search for Higgs boson pair production in $\gamma\gamma bb$ final state in pp collisions at $\sqrt{s} = 13$ TeV with the ATLAS detector

Zihang Jia[1,2]

[1]IHEP, [2]Nanjing University

Outline

- **Motivation**
- **Analysis overview**
- **Event preselection**
- **Event Categorization**
- **Signal and backgound modeling**
- **Results**
- **Summary**

arXiv:2112.11876 (this talk)

JHEP 11 (2018) 040 (ATLAS 36 fb^{-1})

JHEP 03 (2021) 257 (CMS)

ATLAS-PHYS-PUB-2021-031 (HH summary)

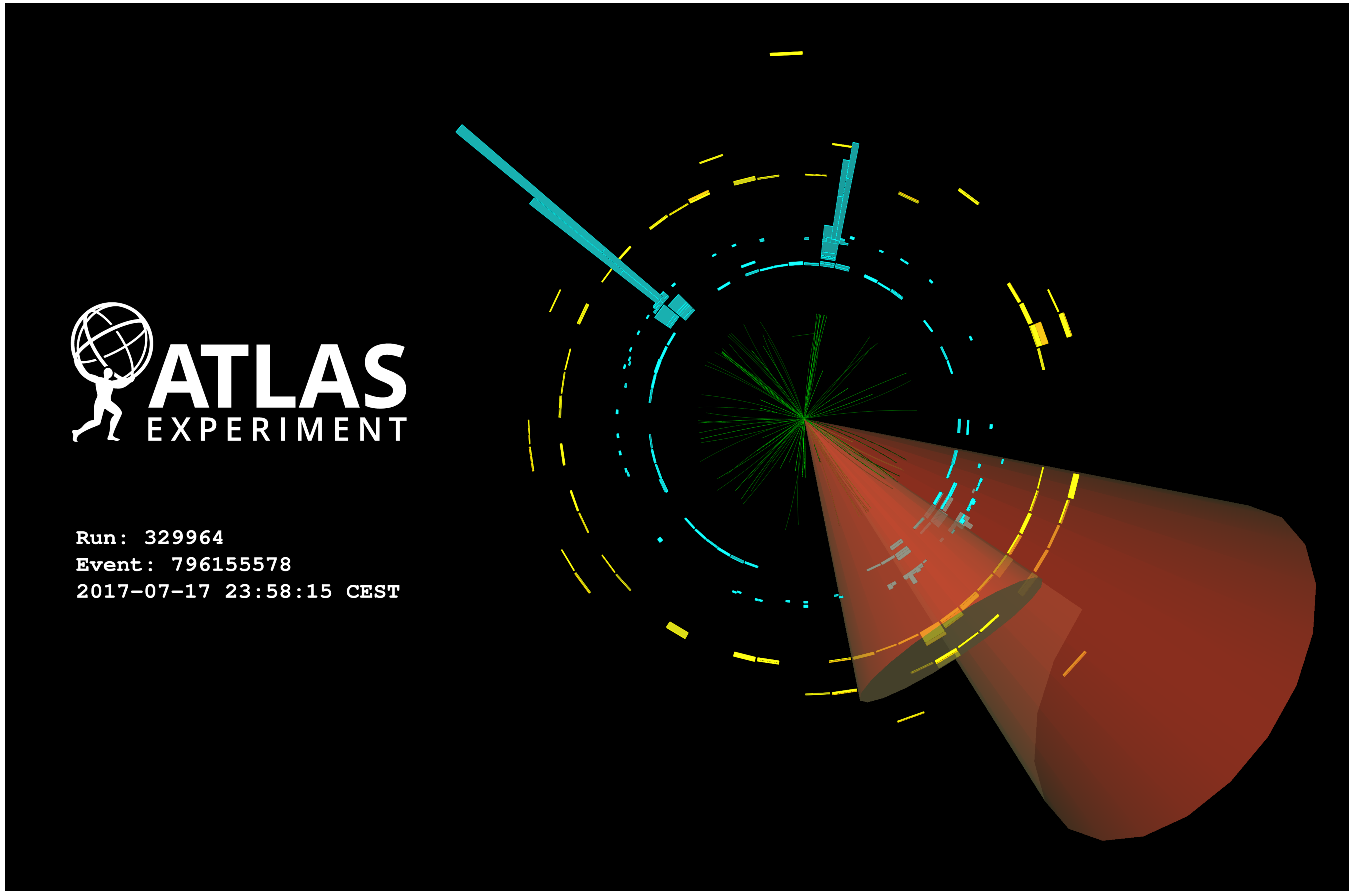

Motivation – Higgs self-coupling

- **The Higgs boson** completes the Standard Model of Particle Physics.
- However, the shape of **the Higgs potential** has yet to be measured.
- We can probe the Higgs potential by measuring the **Higgs self-coupling (λ)**.

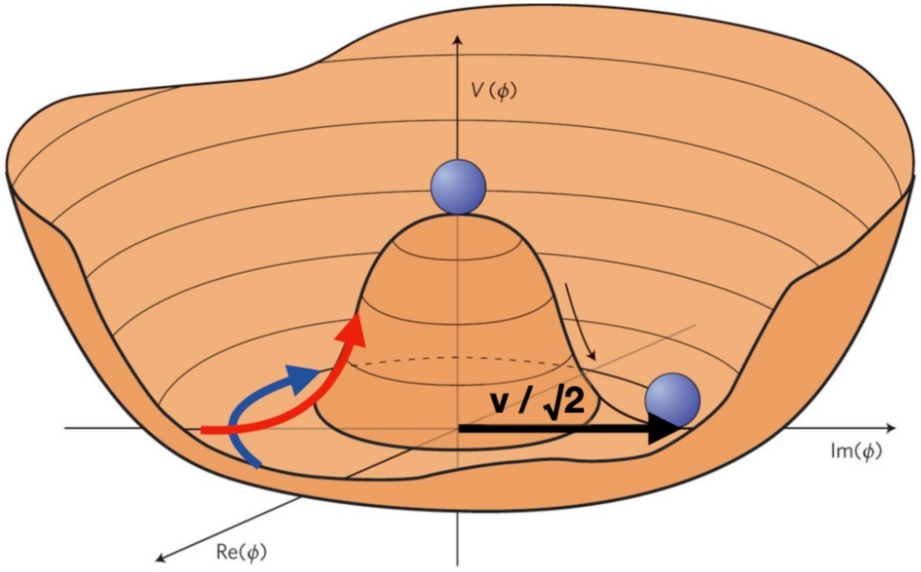

$$V(\phi) = \mu^2\phi^\dagger\phi + \lambda(\phi^\dagger\phi)^2$$
$$= V_0 + \lambda v^2 h^2 + \lambda v h^3 + \frac{1}{4}\lambda h^4$$

Massive scalar
$m_H = \sqrt{2\lambda}v$

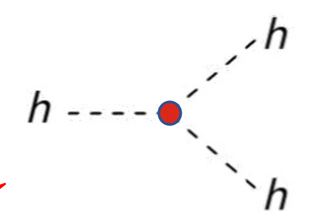

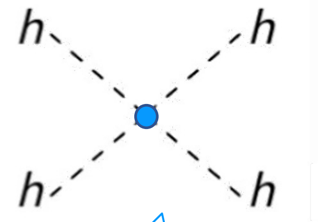

Measuring **HH production** gives us access to the **trilinear** Higgs self−coupling (λ_{HHH})

Out of reach even for HL-LHC

HH production

➢ Measuring **HH production** gives us access to the **trilinear Higgs self-coupling (λ_{HHH}).**

$$\kappa_\lambda = \frac{\lambda_{HHH}}{\lambda_{HHH}^{SM}}$$

SM LHCHWGHH

Gluon-gluon fusion (ggFHH)

Destructive interference, 1000x smaller than single H production.

- σNNLO = **31.02** [fb] @13 TeV, mH = 125.09 GeV

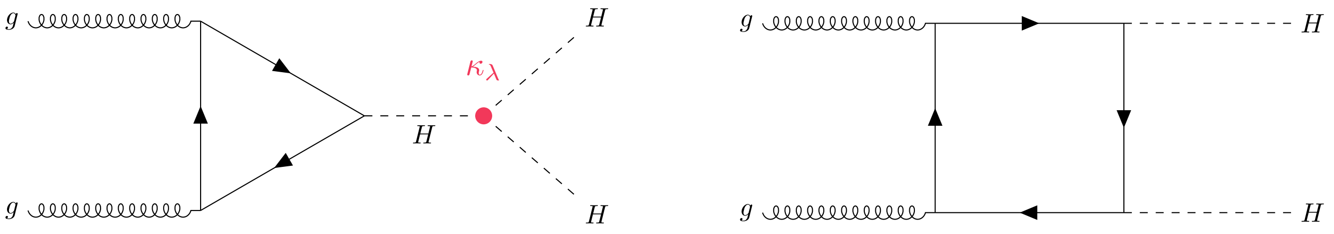

Vector boson fusion (VBFHH)

- σN3LO = **1.723** [fb] @13 TeV, mH = 125.09 GeV

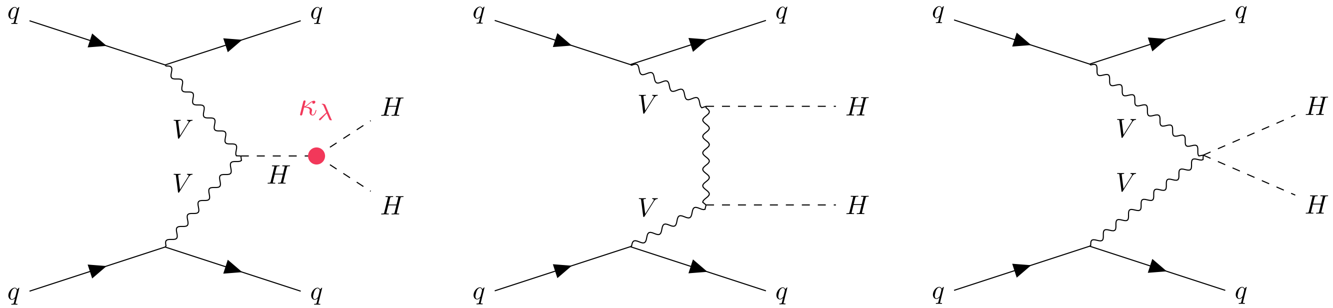

BSM enhancement

Non-resonant HH production

- Anomalous couplings ($\kappa_\lambda \neq 1$, etc.)

Resonant HH production

- X: a narrow-width scalar particle

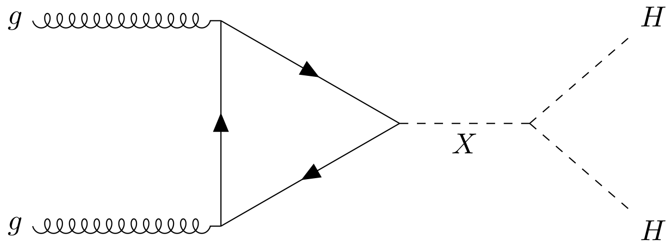

HH$\gamma\gamma bb$ Analysis overview

Search for **Non-resonant** and **Resonant** HH production in $\boldsymbol{\gamma\gamma bb}$ **channel** (full Run2 data, 139 fb^{-1}).

One of the most sensitive HH final states:

- $H \rightarrow bb$: large branching ratio
- $H \rightarrow \gamma\gamma$: excellent photon resolution, clean smoothly falling di-photon background for signal extraction

	bb	WW	ττ	ZZ	γγ
bb	34%				
WW	25%	4.6%			
ττ	7.3%	2.7%	0.39%		
ZZ	3.1%	1.1%	0.33%	0.069%	
γγ	0.26%	0.10%	0.028%	0.012%	0.0005%

HH$\gamma\gamma bb$ Analysis overview

Search for Non-resonant and Resonant HH production in $\boldsymbol{\gamma\gamma bb}$ **channel** (full Run2 data, 139 fb^{-1}).

Main backgrounds

- Non-resonant $\gamma\gamma$ backgrounds
- Single Higgs production

Common Preselection

- 2 identified and isolated photons
- 2 b-tagged jets (77% DL1r b-tagging efficiency)
- < 6 central jets (reject $\boldsymbol{t\bar{t}H}$ events)
- Veto events containing an electron or muon

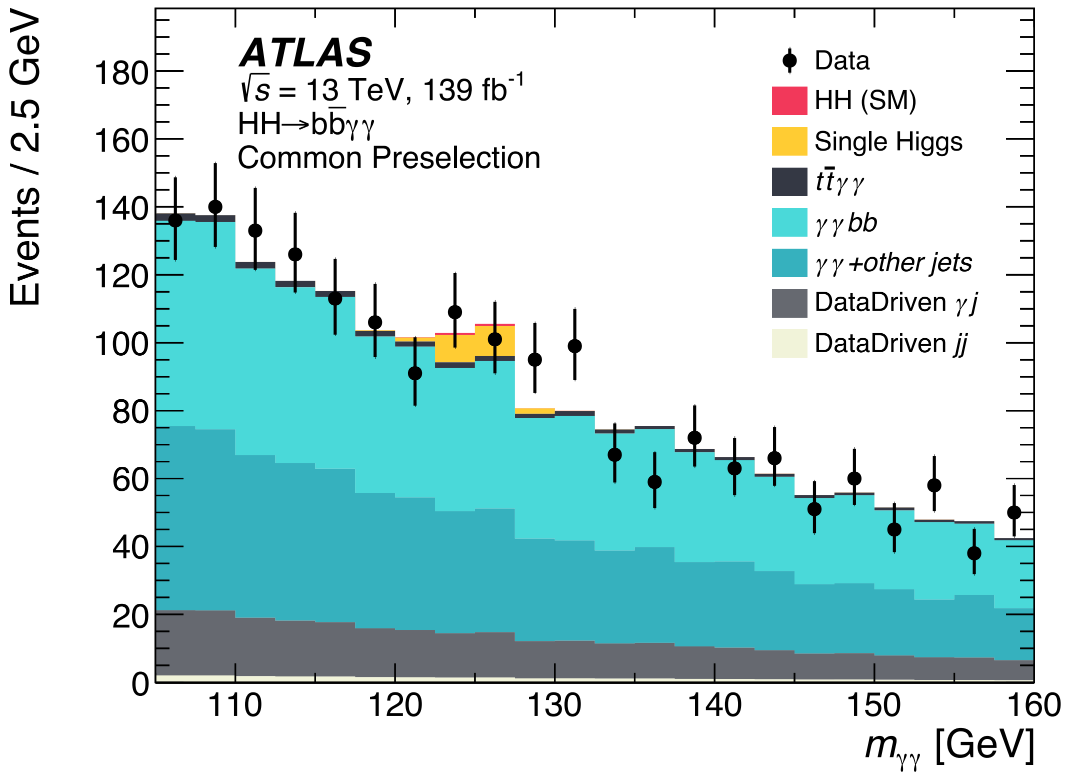

Multivariate method designed to reject background processes

Statistical results obtained from **a fit of** $\boldsymbol{m_{\gamma\gamma}}$ **distribution**

Event preselection

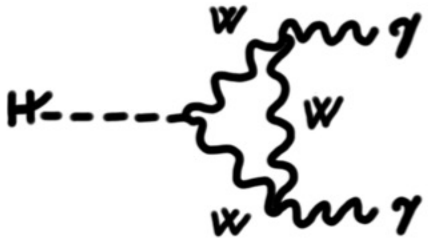

- Photon **identification** (Tight WP)
- Calorimeter- and track-based **isolation** within a cone of $\Delta R = 0.2$

  $E_T^{\text{iso}} < 0.065 \cdot E_T$ and $p_T^{\text{iso}} < 0.05 \cdot E_T$
- $105 < \boldsymbol{m_{\gamma\gamma}} < 160\ GeV$
- $p_T^{\gamma 1}/m_{\gamma\gamma} > 0.35,\ p_T^{\gamma 2}/m_{\gamma\gamma} > 0.25$

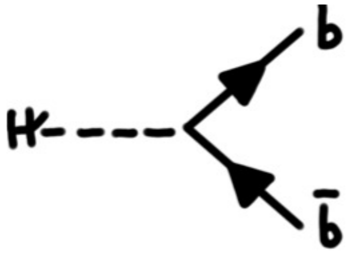

- **DL1r b-tagging** (a deep-learning neural network)

  WP: 77% efficiency
- **Energy correction**
  - **muon-in-jet** correction: muons from semileptonic b-hadron decays
  - $\boldsymbol{p_T}$**-reco** correction: p_T loss due to neutrinos and objects outside of the jet cone

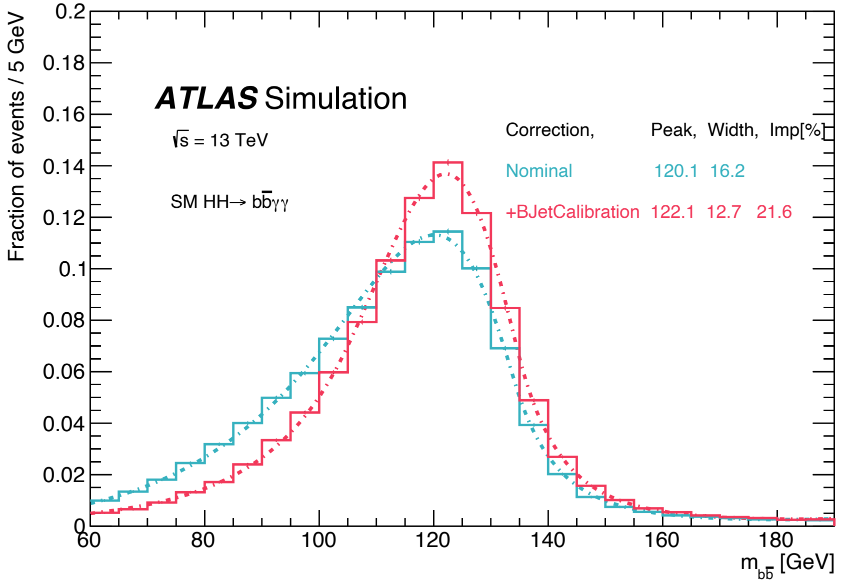

m_{bb} resolution improved by about 22%

Event categorization

Non-resonant analysis: target SM HH → $\gamma\gamma bb$ processes, and possible modifications to κ_λ.

Target only ggF HH production, but VBF HH events also considered as signal

Signal regions defined using $m^*_{\gamma\gamma bb}$ and BDT score

- **Modified invariant mass $m^*_{\gamma\gamma bb} = m_{\gamma\gamma bb} - m_{\gamma\gamma} - m_{bb} + 250\ GeV$**

  Provides cancellation of experimental **resolution** effects

  Spliting into 2 mass regions provide enhanced sensitivity to $\boldsymbol{\kappa_\lambda}$

Step one = 2 HH mass regions

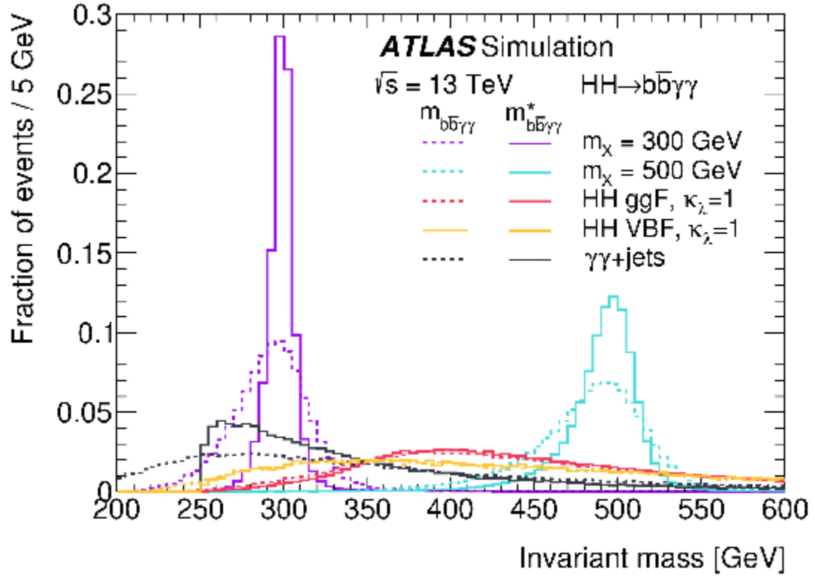

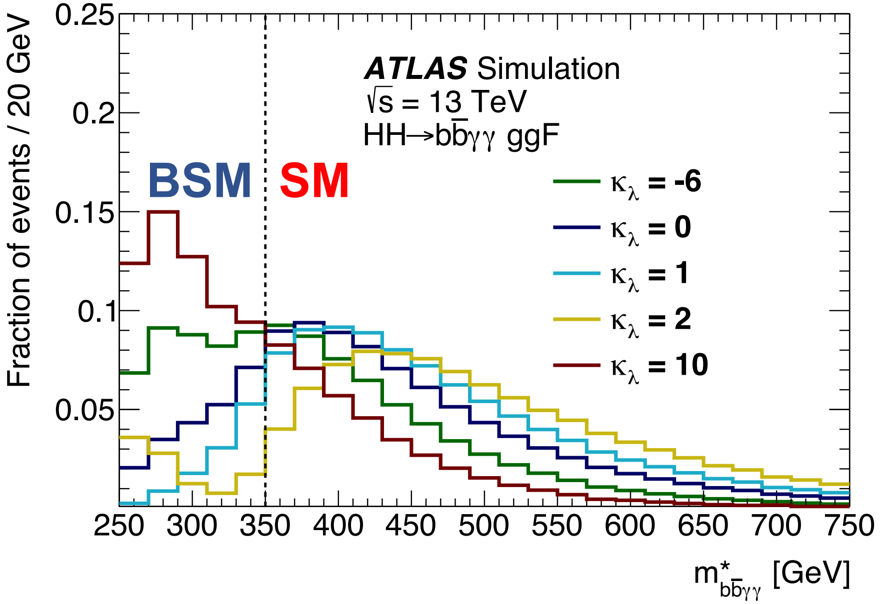

Low mass region
Targeting BSM
$m^*_{\gamma\gamma bb} < 350\ GeV$

High mass region
Targeting SM
$m^*_{\gamma\gamma bb} \geq 350\ GeV$

Event categorization

Non-resonant analysis: target SM HH → $\gamma\gamma bb$ processes, and possible modifications to κ_λ.

Target only ggF HH production, but VBF HH events also considered as signal

Signal regions defined using $m^*_{\gamma\gamma bb}$ and BDT score

- **Boosted Decision Tree, one BDT in each mass region**

  Against $\gamma\gamma$ and single Higgs backgrounds

  BDT trained on photon, jet and missing transverse energy variables

Step two = 4 BDT categories

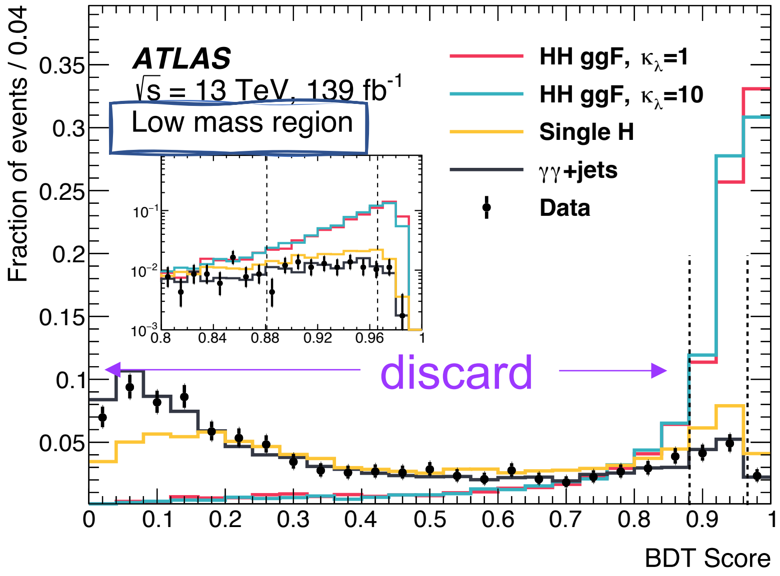

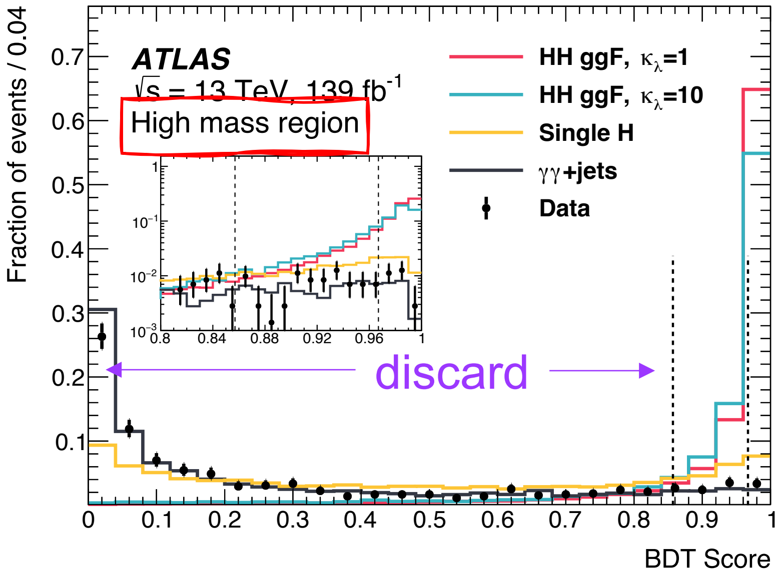

Low mass region
Signal: κ_λ =10 ggF HH
- Loose
- Tight

High mass region
Signal: κ_λ =1 ggF HH
- Loose
- Tight

Boundaries chosen to maximize combined expected significance

Event categorization

Resonant analysis: target $X \to \mathrm{HH} \to \gamma\gamma bb$ processes, with $m_X \in [251, 1000]$ GeV.

Non-resonant SM HH production included as **background**

Signal regions defined using $m^*_{\gamma\gamma bb}$ and BDT score

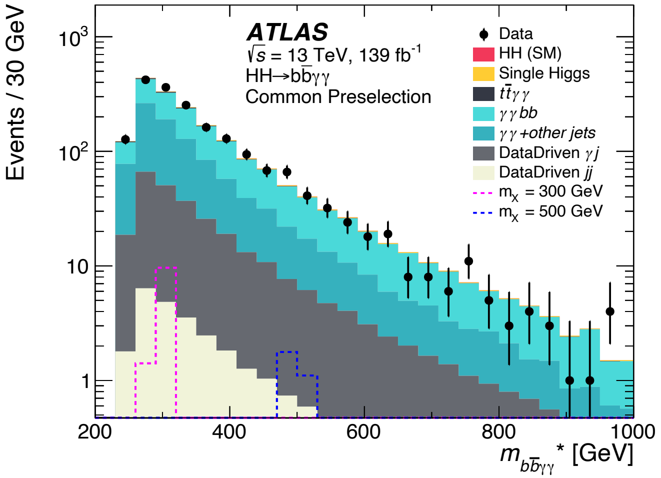

- **Modified invariant mass**

1 category for each m_X

2σ window cut around each m_X

σ = the standard deviation parameter of the Crystal Ball function that best fits the $m^*_{\gamma\gamma bb}$

Relaxed to 4σ for 900 GeV and 1000 GeV mass hypotheses

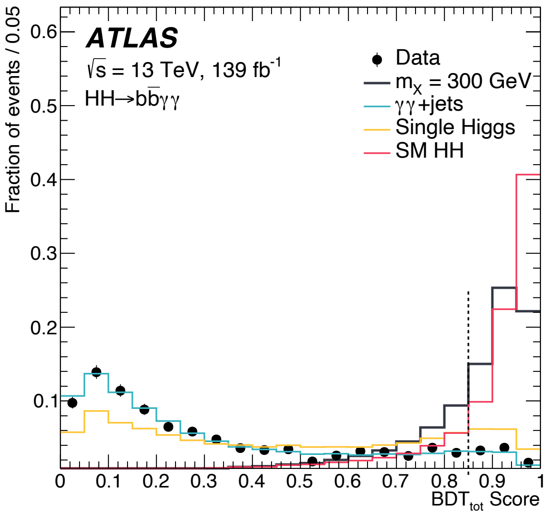

- **Boosted Decision Tree**

Two BDTs against ***γγ+ttγγ*** and **single Higgs** backgrounds respectively

For each m_X, cut on the **combined BDT score**

Shared by all resonance masses to avoid lack of background at high mass

BDTs trained on photon, jet and missing transverse energy variables

Signal and background modeling

The signal and backgrounds are extracted by fitting **analytic functions** to $m_{\gamma\gamma}$ distribution.

➢ Signal parameterization

Modeled with **double sided crystal ball (DSCB) function** derived from **MC**

Non-resonant

- Fit to SM HH signal, model shared with H background
- No sizable dependence on κ_λ is observed

Resonant

- Fit to resonance signals, model shared with SM HH and H background

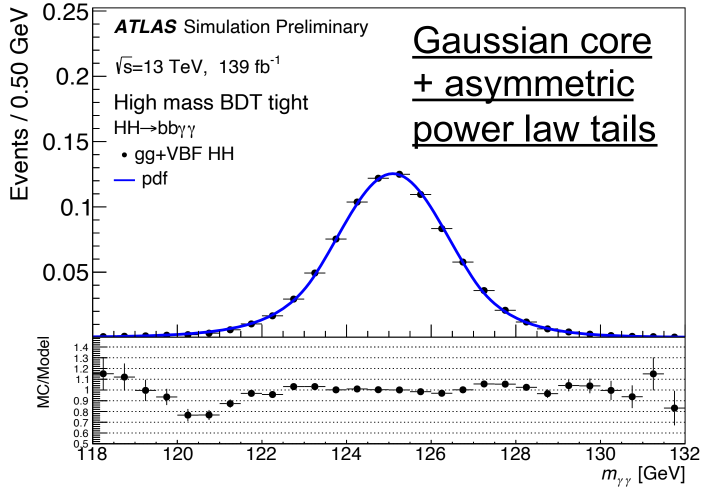

➢ Background parameterization

Modeled with **exponential function**

- Function form determined from **spurious signal** studies
- **spurious signal** = systematic uncertainty assigned to the function **choice**

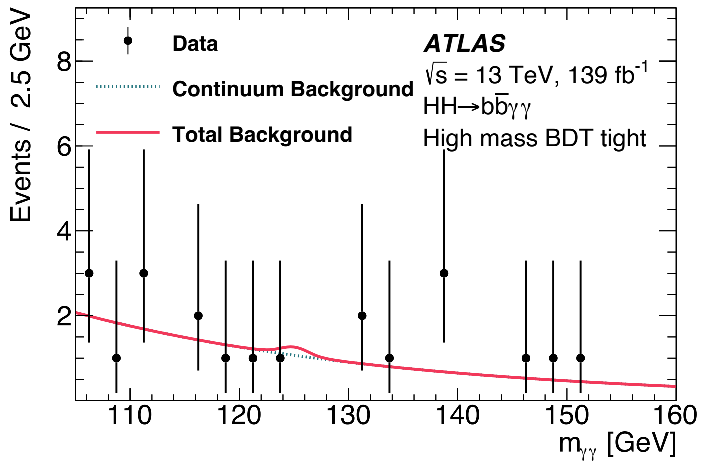

➢ Statistical results obtained from a **maximum-likelihood fit** to the $m_{\gamma\gamma}$ distribution.

Observed (Expected) Results

No signal is observed. **Exclusion limits at 95%CL** are set.

Non-resonant

- $\sigma_{ggF+VBF}(HH)$ **upper limit**: 4.2 x SM (5.7 x SM)
- κ_λ **interval**: [−1.5, 6.7] ([−2.4, 7.7])

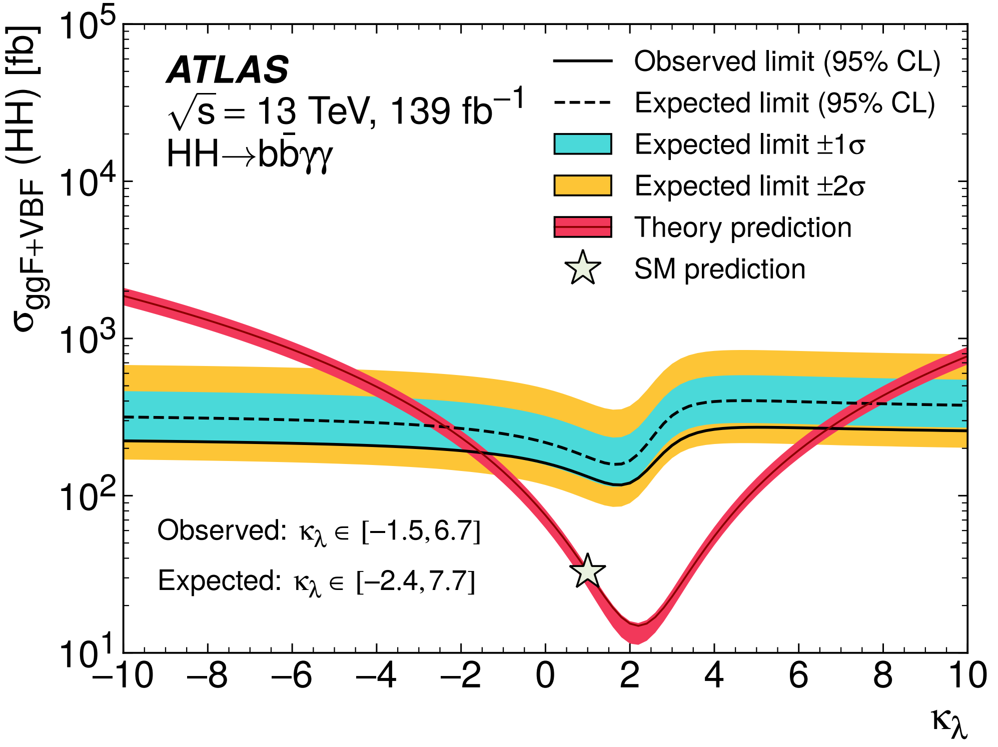

ATLAS 36 fb^{-1} JHEP 11 (2018) 040

$\sigma_{ggF+VBF}(HH)$ **limit:** 22 (28) x SM

κ_λ **interval:** [-8.2, 13.2] ([-8.3, 13.2])

CMS JHEP 03 (2021) 257

$\sigma_{ggF+VBF}(HH)$ **limit:** 7.7 (5.2) x SM

κ_λ **interval:** [-3.3, 8.5] ([-2.5, 8.2])

$\sigma_{ggF+VBF}(HH)$ **upper limit**

improved by a factor of 5 w.r.t 36 fb^{-1}

~2 from increase of luminosity

~rest from analysis strategy

κ_λ **interval** shrinks by a factor of ~2

Observed (Expected) Results

No signal is observed. **Exclusion limits at 95%CL** are set.

Resonant

- $\boldsymbol{\sigma}(\mathbf{X} \rightarrow \mathbf{HH})$ **upper limits** vary between 610 fb and 47 fb (360 fb and 43 fb) in $m_X \in [251, 1000]$ GeV

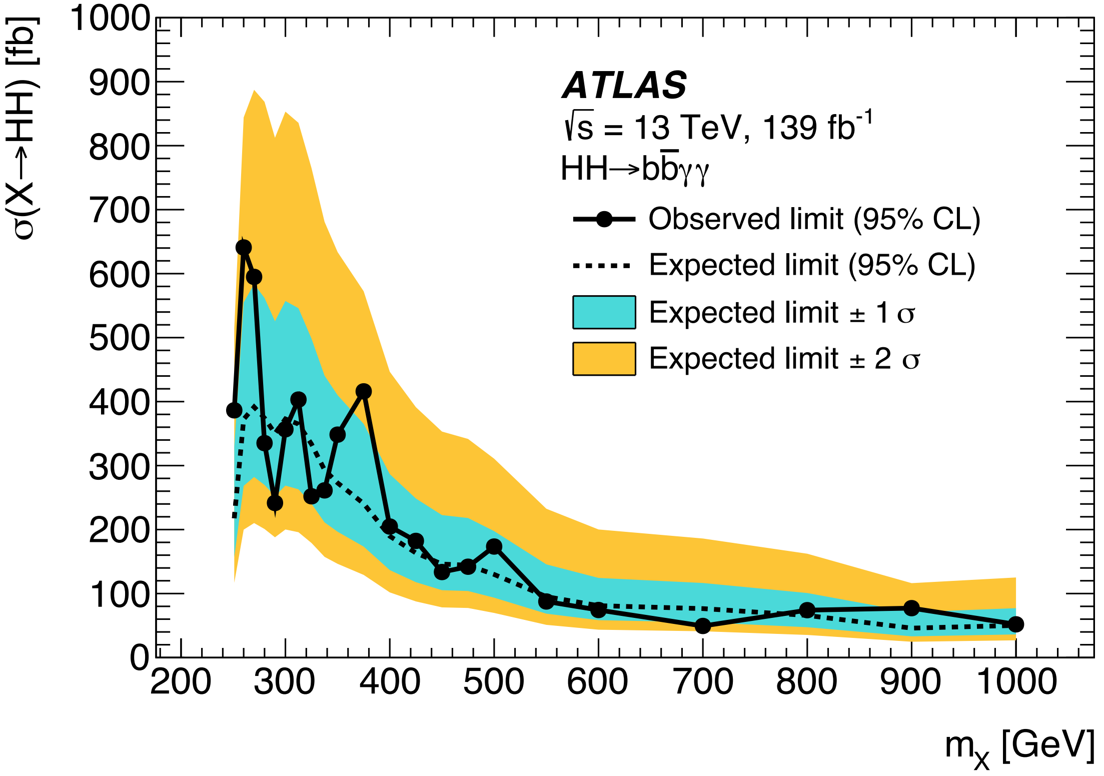

ATLAS 36 fb^{-1} [JHEP 11 (2018) 040]

$\boldsymbol{\sigma}(\mathbf{X} \rightarrow \mathbf{HH})$ upper limits vary between 1.1 pb and 0.12 pb (0.9 pb and 0.15 pb) in $m_X \in [260, 1000]$ GeV

$\boldsymbol{\sigma}(\mathbf{X} \rightarrow \mathbf{HH})$ **upper limits**

improved by a factor of 2-3 depending on the m_X value

~2 from increase of luminosity

~1.2 from analysis strategy

The analyzed mass range expanded to **lower values**

Summary

Searches for non-resonant and resonant HH production are performed in the $bb\gamma\gamma$ final state (139 fb^{-1}).

No significant excess with respect to the SM background expectation is observed.

Improvement compared to the previous ATLAS result based on **36 $\boldsymbol{fb^{-1}}$** data

- Extends the **data set** by more than a factor of 4
- Incorporates a **categorization** based on $m^*_{\gamma\gamma bb}$ and multivariate event selections
- More precise **object reconstruction and calibration**

Status: submitted to PRD

中国科学院高能物理研究所
Institute of High Energy Physics
Chinese Academy of Sciences

NANJING UNIVERSITY 1902

ATLAS EXPERIMENT

Thanks!

HH production

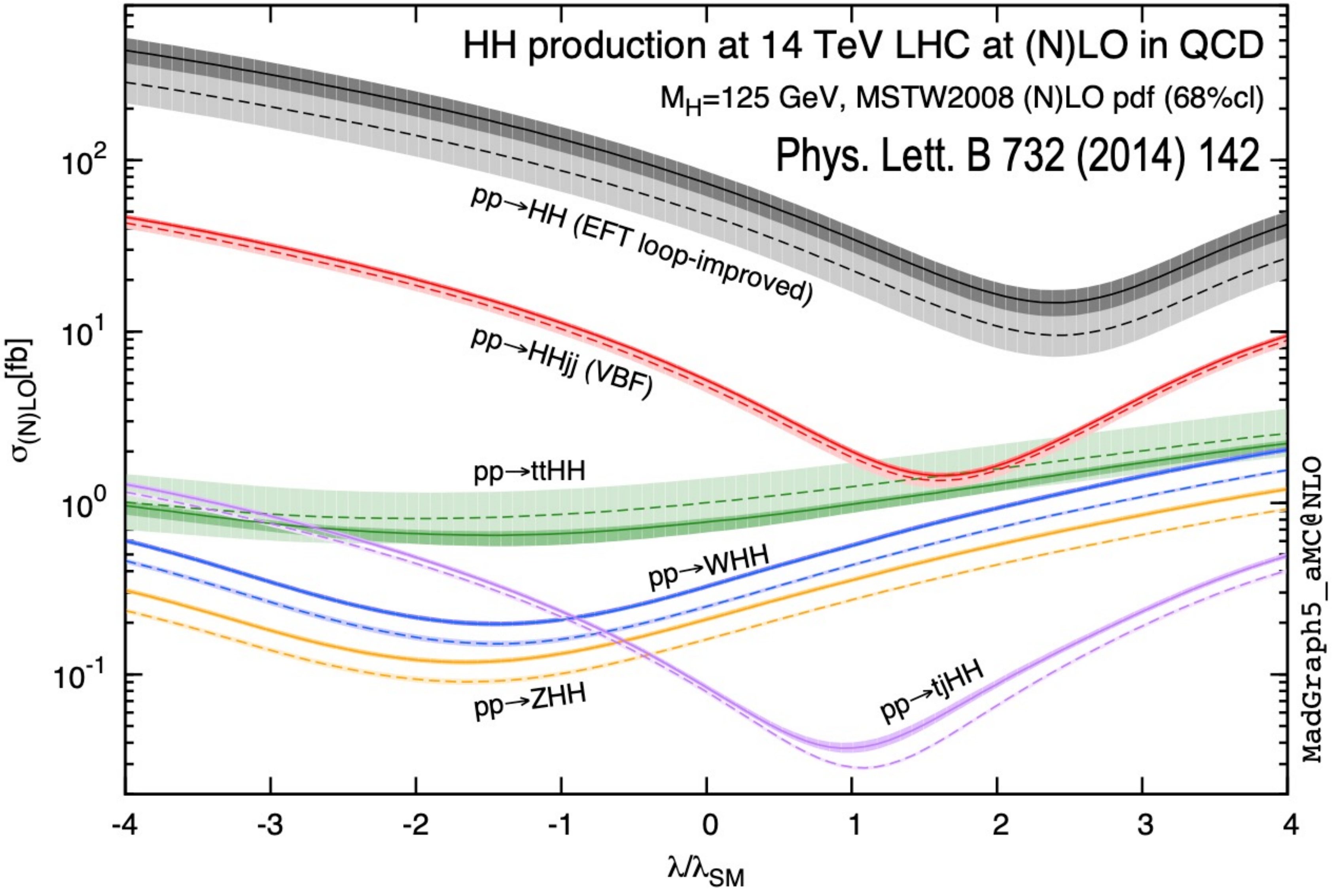

$HH \to b\bar{b}\gamma\gamma$ analysis in a nutshell

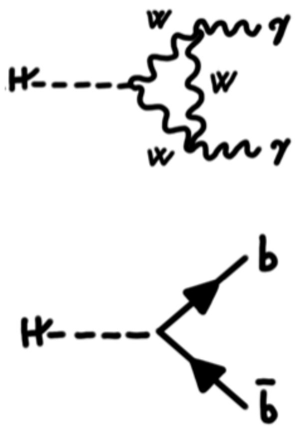

Object selection

Event categorization

MVA approach

4 categories for non-resonant analysis

1 category per m_X for resonant analysis

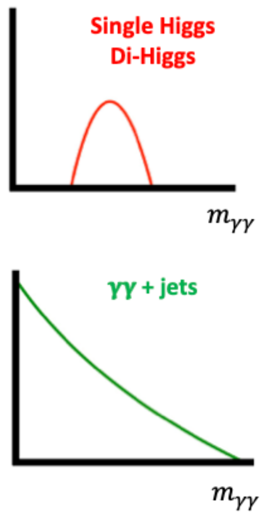

Modelling of discriminant variable

Simultaneous likelihood fit to all categories

SM σ limits and
σ vs k_λ
for non resonant analysis

σ vs m_X
for resonant analysis

Statistically limited with the current dataset

Background Samples

Table 1: Summary of single Higgs boson background samples, split by production modes, and continuum background samples. The generator used in the simulation, the PDF set, and tuned parameters (tune) are also provided.

Process	Generator	PDF set	Showering	Tune
ggF	NNLOPS [65–67] [68, 69]	PDFLHC [42]	Pythia 8.2 [70]	AZNLO [71]
VBF	Powheg Box v2 [39, 66, 72–78]	PDFLHC	Pythia 8.2	AZNLO
WH	Powheg Box v2	PDFLHC	Pythia 8.2	AZNLO
$qq \to ZH$	Powheg Box v2	PDFLHC	Pythia 8.2	AZNLO
$gg \to ZH$	Powheg Box v2	PDFLHC	Pythia 8.2	AZNLO
$t\bar{t}H$	Powheg Box v2 [73–75, 78, 79]	NNPDF3.0nlo [80]	Pythia 8.2	A14 [81]
bbH	Powheg Box v2	NNPDF3.0nlo	Pythia 8.2	A14
$tHqj$	MadGraph5_aMC@NLO	NNPDF3.0nlo	Pythia 8.2	A14
tHW	MadGraph5_aMC@NLO	NNPDF3.0nlo	Pythia 8.2	A14
$\gamma\gamma$+jets	Sherpa v2.2.4 [56]	NNPDF3.0nnlo	Sherpa v2.2.4	–
$t\bar{t}\gamma\gamma$	MadGraph5_aMC@NLO	NNPDF2.3lo	Pythia 8.2	–

Non-resonant BDT variables

Table 2: Variables used in the BDT for the non-resonant analysis. The b-tag status identifies the highest fixed b-tag working point (60%, 70%, 77%) that the jet passes. All vectors in the event are rotated so that the leading photon ϕ is equal to zero.

Variable	Definition
Photon-related kinematic variables	
$p_{\mathrm{T}}/m_{\gamma\gamma}$	Transverse momentum of the two photons scaled by their invariant mass $m_{\gamma\gamma}$
η and ϕ	Pseudo-rapidity and azimuthal angle of the leading and sub-leading photon
Jet-related kinematic variables	
b-tag status	Highest fixed b-tag working point that the jet passes
p_{T}, η and ϕ	Transverse momentum, pseudo-rapidity and azimuthal angle of the two jets with the highest b-tagging score
$p_{\mathrm{T}}^{b\bar{b}}$, $\eta_{b\bar{b}}$ and $\phi_{b\bar{b}}$	Transverse momentum, pseudo-rapidity and azimuthal angle of b-tagged jets system
$m_{b\bar{b}}$	Invariant mass built with the two jets with the highest b-tagging score
H_{T}	Scalar sum of the p_{T} of the jets in the event
Single topness	For the definition, see Eq. (1)
Missing transverse momentum-related variables	
$E_{\mathrm{T}}^{\mathrm{miss}}$ and ϕ^{miss}	Missing transverse momentum and its azimuthal angle

$$\chi_{Wt} = \min\sqrt{\left(\frac{m_{j_1 j_2} - m_W}{m_W}\right)^2 + \left(\frac{m_{j_1 j_2 j_3} - m_t}{m_t}\right)^2},$$

Non-resonant Categorization

$$Z = \sqrt{2 * [(s + b) * \log(1 + s/b) - s]}$$

Low mass region

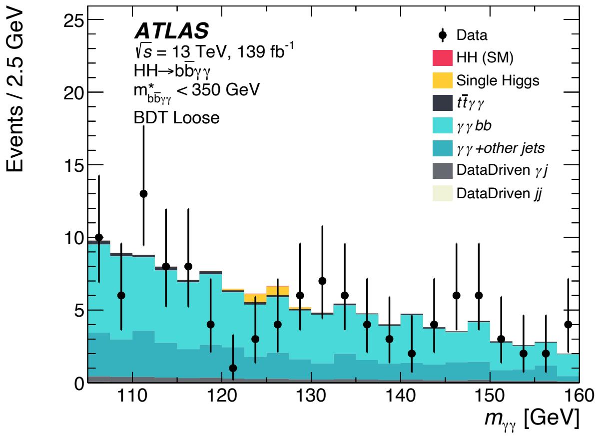

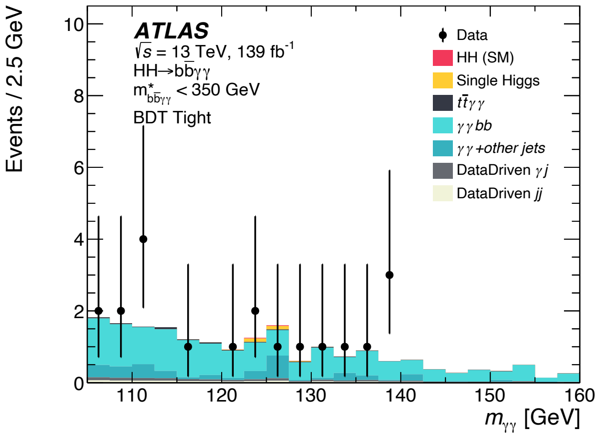

High mass region

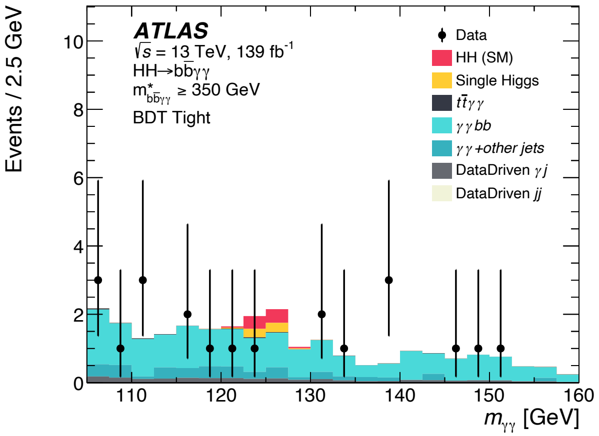

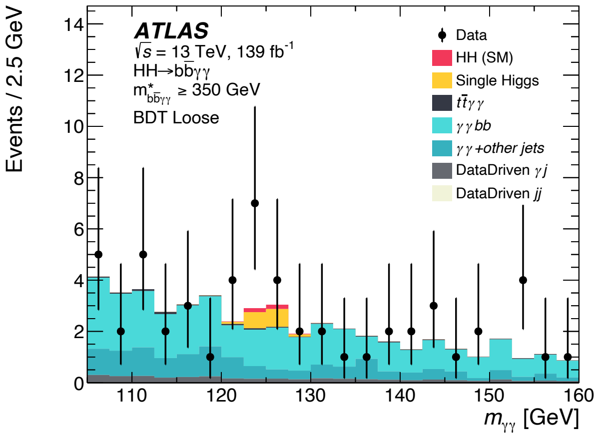

Resonant BDT variables

Table 4: Variables used in the BDT for the resonant analysis. For variables depending on b-tagged jets, only jets b-tagged using the 77% working point are considered as described in Section 4.1.

Variable	Definition
Photon-related kinematic variables	
$p_T^{\gamma\gamma}$, $y^{\gamma\gamma}$	Transverse momentum and rapidity of the di-photon system
$\Delta\phi_{\gamma\gamma}$ and $\Delta R_{\gamma\gamma}$	Azimuthal angular distance and ΔR between the two photons
Jet-related kinematic variables	
$m_{b\bar{b}}$, $p_T^{b\bar{b}}$ and $y_{b\bar{b}}$	Invariant mass, transverse momentum and rapidity of the b-tagged jets system
$\Delta\phi_{b\bar{b}}$ and $\Delta R_{b\bar{b}}$	Azimuthal angular distance and ΔR between the two b-tagged jets
N_{jets} and $N_{b-\text{jets}}$	Number of jets and number of b-tagged jets
H_T	Scalar sum of the p_T of the jets in the event
Photons and jets-related kinematic variables	
$m_{b\bar{b}\gamma\gamma}$	Invariant mass built with the di-photon and b-tagged jets system
$\Delta y_{\gamma\gamma,b\bar{b}}$, $\Delta\phi_{\gamma\gamma,b\bar{b}}$ and $\Delta R_{\gamma\gamma,b\bar{b}}$	Distance in rapidity, azimuthal angle and ΔR between the di-photon and the b-tagged jets system

$$\text{BDT}_{\text{tot}} = \frac{1}{\sqrt{C_1^2 + C_2^2}} \sqrt{C_1^2 \left(\frac{\text{BDT}_{\gamma\gamma} + 1}{2}\right)^2 + C_2^2 \left(\frac{\text{BDT}_{\text{Single}H} + 1}{2}\right)^2}$$

- **2-stage optimization**
  1. Maximize significance for each resonance
     - Different coefficients and BDT scores
  2. Select coefficients providing a significance within 5% from the maximum value, for each resonance
     - A common C_1 = 0.65 coefficient is found, individual BDT cuts are used

Signal modeling - DSCB

A Gaussian core + asymmetric power law tails

$$f_{\text{DSCB}}(m_{\gamma\gamma}) = N \times \begin{cases} e^{-t^2/2} & \text{if } -\alpha_{low} \leq t \leq \alpha_{high} \\ \dfrac{e^{-\frac{1}{2}\alpha_{low}^2}}{\left[\frac{1}{R_{low}}\left(R_{low} - \alpha_{low} - t\right)\right]^{n_{low}}} & \text{if } t < -\alpha_{low} \\ \dfrac{e^{-\frac{1}{2}\alpha_{high}^2}}{\left[\frac{1}{R_{high}}\left(R_{high} - \alpha_{high} + t\right)\right]^{n_{high}}} & \text{if } t > \alpha_{high} \end{cases}$$

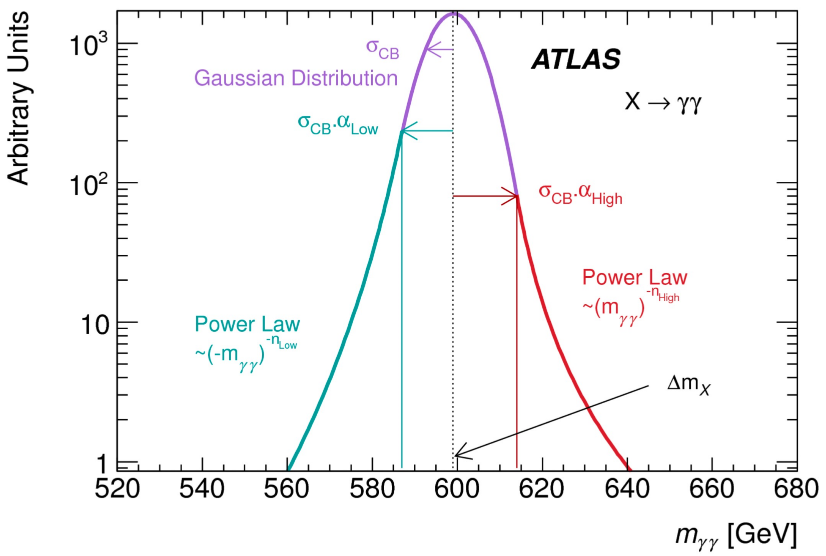

where N is a normalization factor and the six parameters are

- μ_{CB} and σ_{CB} describe the mean and the width of the Gaussian core, which are combined in $t = \left(m_{\gamma\gamma} - \mu_{\text{CB}}\right)/\sigma_{\text{CB}}$;
- α_{low} and α_{high} are the positions of the transitions with respect to μ_{CB} from the Gaussian core to power-law tails, in unit of σ_{CB}, on the low and high mass sides respectively;
- n_{low} and n_{high} are the exponents of the low and high mass tails. With the α's, they define $R_{low} = \frac{n_{low}}{\alpha_{low}}$ and R_{high} similarly.

non-Gaussian tails can arise from experimental effects, such as photon energy mismeasurements.

Diphoton background decomposition

- Reconstructed $\gamma\gamma$ events is mainly composed of $\gamma\gamma$, γ-jets and jet-jet events, where **the jet(s) fake(s) a real photon.**
- The 2x2D sideband method is developed using the discriminating power of **photon identification and isolation criteria.**
- The event yields in the signal region and the 15 sidebands can be expressed as **functions** of the photon efficiencies, jet fake rates and correlation coefficients.

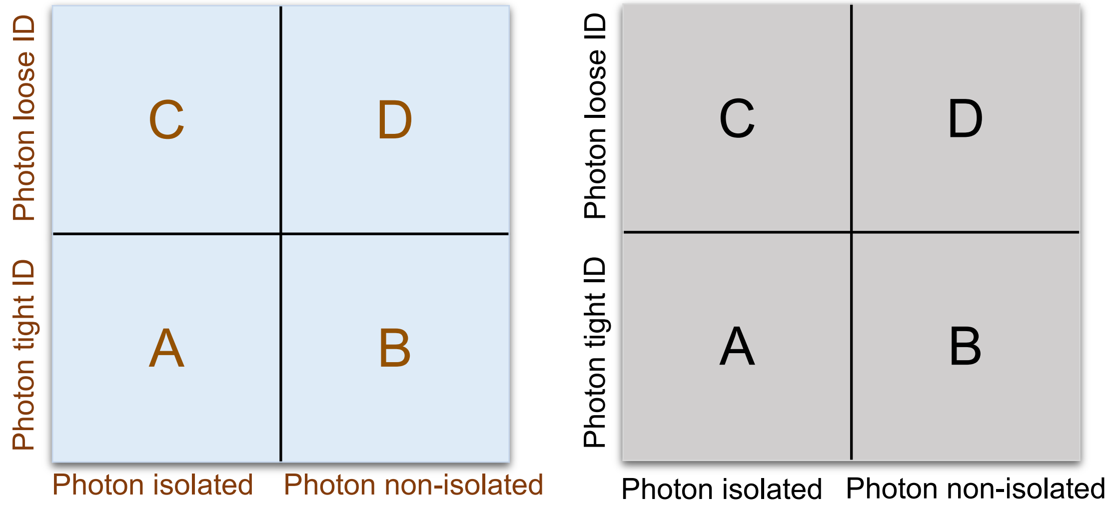

Leading object   Sub-leading object

CC	CD	DC	DD
CA	CB	DA	DB
AC	AD	BC	BD
AA	AB	BA	BB

Reference

Suffers from **low statistics**, not used in constructing the background templates for the spurious signal procedure.

Spurious signal

Spurious signal: a bias estimated from a **signal + background** fit to a **background-only** MC template.

$$N_{sp} = \max_{121<m_H<129\,GeV} |N_s(m_H)|$$

➢ **Selection criteria:**

- ☐ N_{sp} < 20% of the data's statistical uncertainty + 2 × the MC background template statistical uncertainty
- ☐ must satisfy a simple χ^2 requirement in a background-only fit to the MC template: $p-value(\chi^2) > 1\%$

- **The least number of parameters** is preferred.
- The **smaller systematic uncertainty** (spurious signal) is preferred.

Wald tests show that the data do not prefer a higher degree functional form with respect to the exponential form.

Systematic uncertainties

In general the analysis is almost completely **statistically dominated** with the Run 2 dataset

		Relative impact of the systematic uncertainties [%]	
Source	Type	Nonresonant analysis HH	Resonant analysis m_X = 300 GeV
Experimental			
Photon energy resolution	Norm. + Shape	0.4	0.6
Jet energy scale and resolution	Normalization	< 0.2	0.3
Flavor tagging	Normalization	< 0.2	0.2
Theoretical			
Factorization and renormalization scale	Normalization	0.3	< 0.2
Parton showering model	Norm. + Shape	0.6	2.6
Heavy-flavor content	Normalization	0.3	< 0.2
$\mathcal{B}(H \to \gamma\gamma, b\bar{b})$	Normalization	0.2	< 0.2
Spurious signal	Normalization	3.0	3.3

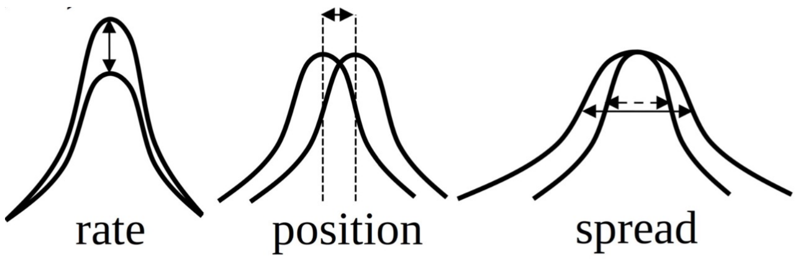

Statistical framework

➢ The results of the analysis are obtained from a **maximum-likelihood fit** of the $m\gamma\gamma$ distribution.

Likelihood

$$\mathcal{L} = \prod_c \left(\text{Pois}(n_c | N_c(\boldsymbol{\theta})) \cdot \prod_{i=1}^{n_c} f_c(m^i_{\gamma\gamma}, \boldsymbol{\theta}) \cdot G(\boldsymbol{\theta}) \right)$$

Event parameterization

$$N_c(\boldsymbol{\theta}) = \mu \cdot N_{HH,\text{c}}(\boldsymbol{\theta}^{\text{yield}}_{HH}) + N^{\text{res}}_{\text{bkg,c}}(\boldsymbol{\theta}^{\text{yield}}_{\text{res}}) + N_{\text{SS,c}} \cdot \boldsymbol{\theta}^{\text{SS,c}} + N^{\text{non-res}}_{\text{bkg,c}}$$

Model PDF

$$f_c(m_{\gamma\gamma}, \boldsymbol{\theta}) = [\mu \cdot N_{HH,\text{c}}(\boldsymbol{\theta}^{\text{yield}}_{HH}) \cdot f_{HH,\text{c}}(m_{\gamma\gamma}, \boldsymbol{\theta}^{\text{shape}}_{HH}) + N^{\text{res}}_{\text{bkg,c}}(\boldsymbol{\theta}^{\text{yield}}_{\text{res}}) \cdot f^{\text{res}}_{\text{bkg,c}}(m_{\gamma\gamma}, \boldsymbol{\theta}^{\text{shape}}_{\text{res}}) + N_{\text{SS,c}} \cdot \boldsymbol{\theta}^{\text{SS,c}}_{HH} \cdot f_{HH,\text{c}}(m_{\gamma\gamma}, \boldsymbol{\theta}^{\text{shape}}_{HH}) + N^{\text{non-res}}_{\text{bkg,c}} \cdot f^{\text{non-res}}_{\text{bkg,c}}(m_{\gamma\gamma}, \boldsymbol{\theta}^{\text{shape}}_{\text{non-res}})] / N_c(\boldsymbol{\theta}^{\text{yield}}_{\text{non-res}}),$$

Statistical framework

- The measurement of the parameter of interest is carried out using a statistical test based on the **profile likelihood ratio**

the profile likelihood ratio

$$\Lambda(\mu) = \frac{\mathcal{L}(\mu, \hat{\hat{\boldsymbol{\theta}}}(\mu))}{\mathcal{L}(\hat{\mu}, \hat{\boldsymbol{\theta}})}$$

the profile-likelihood-ratio-based test statistic

$$\tilde{q}_\mu = \begin{cases} -2\ln \frac{\Lambda(\mu, \hat{\hat{\boldsymbol{\theta}}}(\mu))}{\Lambda(0, \hat{\hat{\boldsymbol{\theta}}}(0))} & \hat{\mu} < 0, \\ -2\ln \frac{\Lambda(\mu, \hat{\hat{\boldsymbol{\theta}}}(\mu))}{\Lambda(\hat{\mu}, \hat{\boldsymbol{\theta}}(\mu))} & 0 \le \hat{\mu} \le \mu, \\ 0 & \hat{\mu} > \mu. \end{cases}$$

κ_λ reweighting for ggF HH samples

Common HH procedure. The method derives the **scale factors as a function of $\boldsymbol{\kappa_\lambda}$** in **bins of $\boldsymbol{m_{HH}}$** by performing a **linear combination** of samples generated at $\kappa_\lambda = 0, 1, 20$.

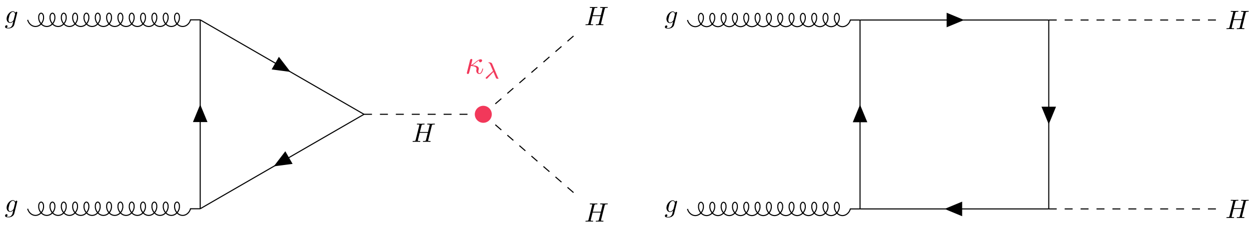

$$\mathcal{A}(\kappa_t, \kappa_\lambda) = \kappa_t^2 \mathcal{A}_1 + \kappa_t \kappa_\lambda \mathcal{A}_2$$

$$\sigma_{\mathrm{ggF}}(pp \to HH) \propto \int \kappa_t^4 \left[|\mathcal{A}_1|^2 + 2\left(\frac{\kappa_\lambda}{\kappa_t}\right) \Re(\mathcal{A}_1^* \mathcal{A}_2) + \left(\frac{\kappa_\lambda}{\kappa_t}\right)^2 |\mathcal{A}_2|^2 \right]$$

$$\sigma(\kappa_t = 1, \kappa_\lambda = 0) \sim |\mathcal{A}_1|^2$$

$$\sigma(\kappa_t = 1, \kappa_\lambda = 1) \sim |\mathcal{A}_1|^2 + 2\Re \mathcal{A}_1^* \mathcal{A}_2 + |\mathcal{A}_2|^2$$

$$\sigma(\kappa_t = 1, \kappa_\lambda = 20) \sim |\mathcal{A}_1|^2 + 2 \cdot 20 \Re \mathcal{A}_1^* \mathcal{A}_2 + 20^2 |\mathcal{A}_2|^2$$

$$\sigma(\kappa_t, \kappa_\lambda) \sim \kappa_t^2 \left[\left(\kappa_t^2 + \frac{\kappa_\lambda^2}{20} - \frac{399}{380} \kappa_\lambda \kappa_t \right) |S(1,0)|^2 + \left(\frac{40}{38} \kappa_\lambda \kappa_t - \frac{2}{38} \kappa_\lambda^2 \right) |S(1,1)|^2 + \left(\frac{\kappa_\lambda^2 - \kappa_\lambda \kappa_t}{380} \right) |S(1,20)|^2 \right]$$

$$d\sigma/dm_{HH} = A(m_{HH}) + B(m_{HH})\kappa_\lambda + C(m_{HH})\kappa_\lambda^2$$

HH summary

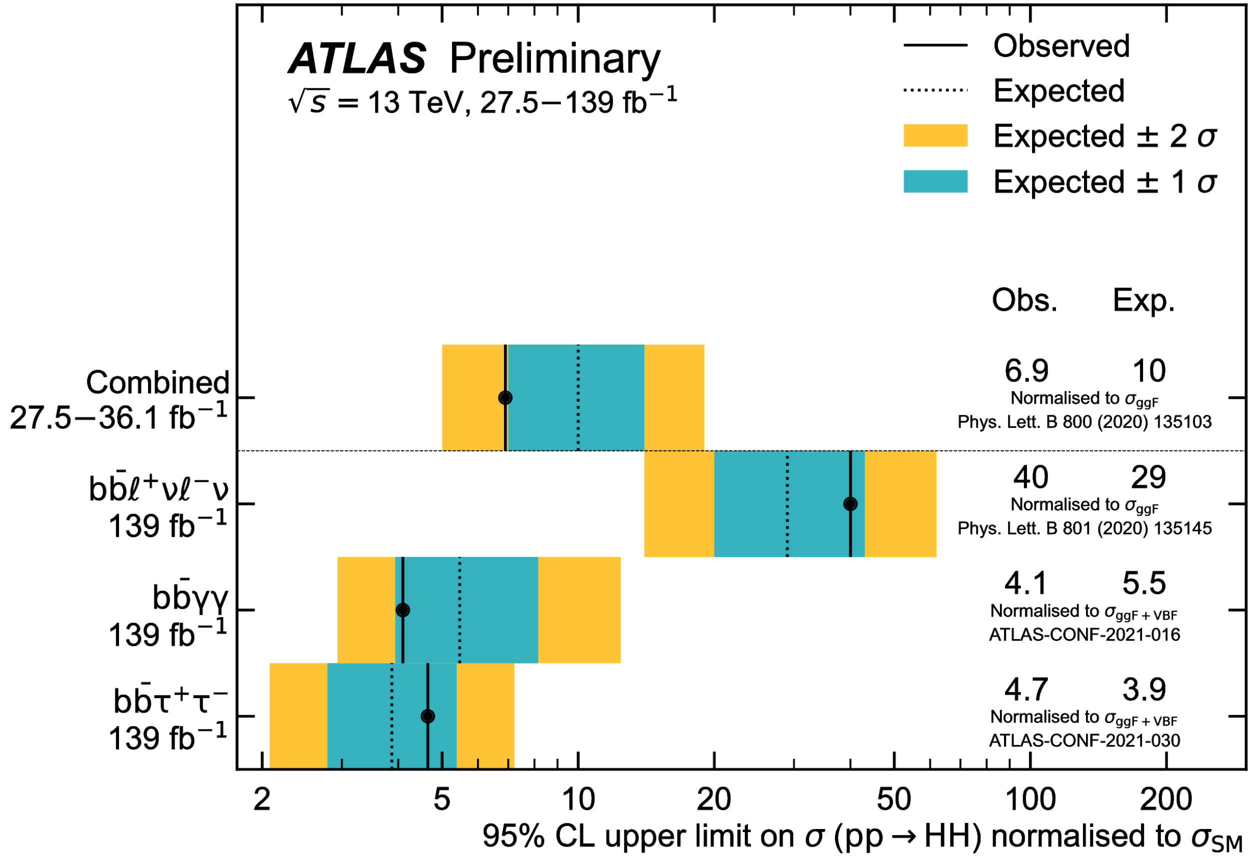

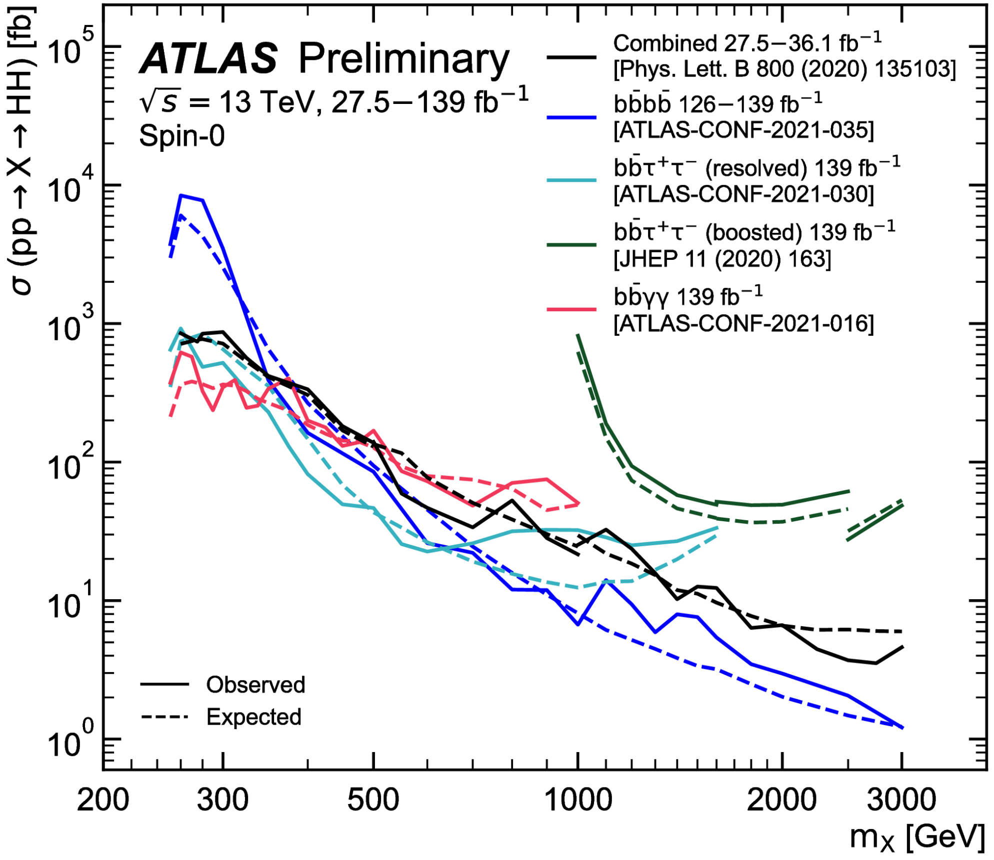

good sensitivity at low resonant masses